Journal of Chromatography, 151 (1978) 95–112

CHROM. 10,700

THEORY OF CHROMATOGRAPHY OF RIGID MOLECULES ON HYDROXYAPATITE COLUMNS WITH SMALL LOADS

IV. ESTIMATION OF THE ADSORPTION ENERGY OF NUCLEOSIDE POLYPHOSPHATES

TSUTOMU KAWASAKI

Laboratoire de Génétique Moléculaire, Institut de Recherche en Biologie Moléculaire, Faculté des Sciences, Paris 5° (France)

(Received June 17th, 1977)

SUMMARY

Taves and Reedy postulated that phosphate ions are adsorbed at hydroxyl positions on the surface of hydroxyapatite, and proposed a model for the adsorption of tripolyphosphate on the crystal surface. On the basis of this model and the hypothesis that a hydroxyl position on the crystal surface corresponds to a chromatographic C site, the experimental chromatogram for a mixture of AMP, ADP, ATP and adenosine tetraphosphate obtained by Bernardi was analysed by using the theory developed in an earlier paper in this series. It was estimated that the energy of adsorption on a C site for a univalent phosphate group on the polyphosphate chain of nucleoside polyphosphate is 0.9–1 kcal/mole and that the adenosine group of the molecule covers at most only one crystal site. Some other experimental parameters were also evaluated. The reasonable results obtained in the calculation strongly support the hypothesis of the one-to-one correspondence between a hydroxyl position and a chromatographic C site and the model of Taves and Reedy.

INTRODUCTION

A model of the surface structure of hydroxyapatite (HA) was proposed by Taves and Reedy[1] on the basis of a comparison of the crystallographic structure of HA with the structure of octacalcium phosphate (OCP). OCP contains alternating sheets of an apatite structure[2–4] and a loose water-rich layer, which are parallel to the $(\vec{b}, \vec{c})$ plane of the crystal structure[5,6]. The apatite structure in OCP consists of a monolayer of apatite cells, each of the four edges (corresponding to four 6_3 axes[2,3]) of each apatite cell being on the interface with the water-rich layer. Two positions that would be occupied by OH^- ions in the HA structure are involved in this edge; with OCP, however, these positions are replaced by a water molecule and an HPO_4^{2-} ion (see Fig. 1 and refs. 5 and 6). Whether the crystal grows as OCP or HA appears to depend on whether one of these positions is occupied by a phosphate ion or a hydroxyl ion[6].

The fact that these positions are on the interface between the HA cell and the water-rich layer in the case of OCP suggests that the crystal surfaces [corresponding to $(\vec{a}, \vec{c})$ and $(\vec{b}, \vec{c})$ planes] of HA must also involve these positions. The fact that OCP grows more rapidly than HA, even though the latter is more stable, is consistent with this hypothesis[6]. Under physiological conditions where the hydroxyl ions in the surrounding solution would be present in much lower concentration than the phosphate ions, these positions on the surfaces of HA must be occupied by many more phosphate ions than hydroxyl ions[6]. Further, it can be estimated that the HPO_4^{2-} ion on the crystal surface (or on the interface in the case of OCP) has oxygen–calcium distances of 2.37, 2.39 and 2.63 Å and a hydrogen bond length of 2.46 Å (see Fig. 1), whereas a hydroxyl in the corresponding position would have only two comparable calcium–oxygen distances and only a weak hydrogen bond, if any[6]. The crystal growth of HA must be blocked when the surface hydroxyl positions are taken up by phosphate ions[1,6]. If unfilled, these positions form grooves running parallel to the $\vec{c}$ axis and these can be considered as adsorption sites for phosphate ions[1,6]. It is probable that the hydroxyl position corresponds to a chromatographic C site, using the nomenclature of earlier

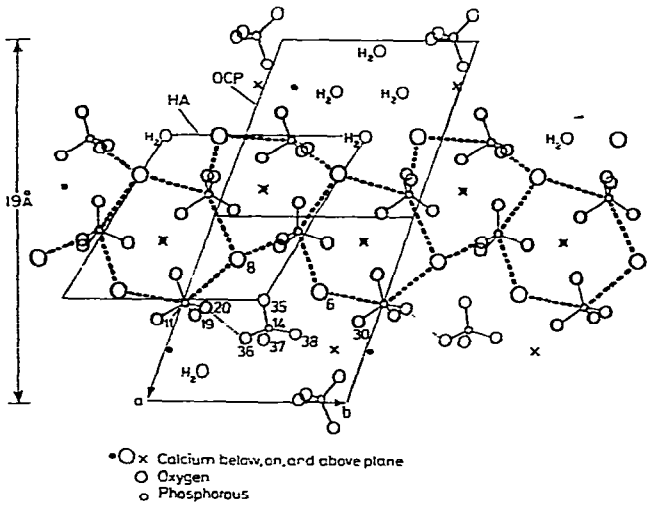

Fig. 1. Atomic positions in OCP on an $(\vec{a}, \vec{b})$ plane at the level of $z \approx 1/4$. The ions connected by dashed lines are those that are common to HA and OCP, and constitute an apatite layer (parallel to $\vec{b}$) inserted between water-rich layers. Two half-unit cells are shown for OCP and one for HA. The key positions are at the corners of the "HA unit cell". To allow the crystal to grow as HA, these must be OH^- ions instead of the H_2O and HPO_4^{2-} shown here (for HPO_4^{2-}, only one of them is shown). This hydrogen phosphate ion (with phosphorus No. 14) has oxygen–calcium distances of 2.37, 2.39 and 2.63 Å and a hydrogen bond length of 2.46 Å (between atoms 20 and 36). A hydroxyl in the position of oxygen No. 35 would have only two comparable calcium–oxygen distances, and only a weak hydrogen bond, if any. In both OCP and HA, two types of the plane alternate along the $\vec{c}$ axis separated by $|\vec{c}|/2$ or 3.44 Å at $z \approx 1/4$ (shown in the figure) and $z \approx 3/4$, respectively, that is, in the second plane of the unit cell the HA cell contents including the water and hydrogen phosphate are located in a reversed or 180° rotated manner. If the corners of the "HA unit cell" are unfilled, they form grooves running in the lateral surfaces parallel to the $\vec{c}$ axis. (This figure is reproduced from ref 1, with the permission of Dr. D. R. Taves).

papers[7–9] in this series (see Fig. 2). It was suggested by Kawasaki (Appendix I in ref. 7) that the C site exists on the side faces of the crystal or the lateral faces parallel to the $\vec{c}$ axis, which is consistent with the hypothesis that a C site corresponds to a hydroxyl position on the ($\vec{a}$, $\vec{c}$) and the ($\vec{b}$, $\vec{c}$) surfaces of HA.

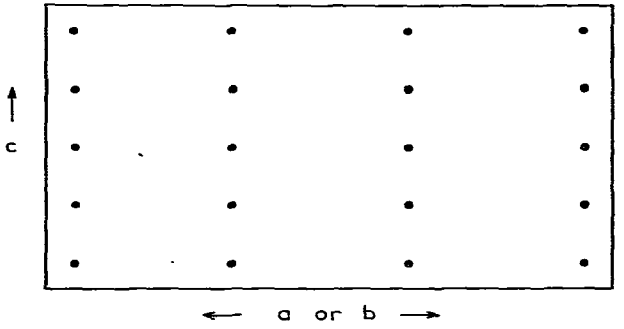

Fig. 2. Schematic representation of hydroxyl positions on the ($\vec{a}$, $\vec{c}$) or the ($\vec{b}$, $\vec{c}$) surface of HA. The minimal interval between the positions in the $\vec{a}$ or $\vec{b}$ direction (*i.e.*, $|\vec{a}|$ or $|\vec{b}|$) and the interval in the $\vec{c}$ direction (*i.e.*, $|\vec{c}|/2$) are 9.42 and 3.44 Å, respectively (*cf.*, Fig. 1 and see refs. 2–4). It is probable that a hydroxyl position constitutes a chromatographic C site (see text). This figure can be compared with Fig. 3 in an earlier paper[7] in which the possible arrangement of P sites is shown.

It was shown by Krane and Glimcher[10] that various nucleoside tri- and diphosphates as well as inorganic pyrophosphate are adsorbed on synthetic apatite crystals at physiological temperature and pH and that the terminal phosphorus atom of the bound nucleotide is transferred, after incubation for several minutes, to a crystal surface phosphate with the formation of pyrophosphate on the crystal and the respective di- and monophosphate (for the transphosphorylation, see Discussion). In connection with this finding, it was proposed by Taves and Reedy[1] that tripolyphosphate is likely to be adsorbed on the surface of HA with its long axis parallel to the $\vec{c}$ axis of the crystal and that the three phosphate groups of the molecule occupy three successive hydroxyl positions [separated by 3.44 Å (see Fig. 2)] of HA, for the following reasons. Firstly, there is a very good fit when the ions on the hydroxyl positions are replaced by a tripolyphosphate, while nothing comparable is found for other orientations or replacements. Secondly, the displacement of HPO_4^{2-} from a hydroxyl position would be much easier than the displacement of a structural phosphate. The former has three favourable electrostatic distances, 2.37–2.63 Å, while the latter has five or more good electrostatic distances.

This model is firmly supported by the HA chromatography of nucleoside mono-, di-, tri- and tetraphosphates and their derivatives carried out by Bernardi[11]. The non-phosphorylated derivatives were not retained by HA equilibrated with 1 m*M* potassium phosphate buffer (pH 6.8); monophosphates were eluted by 1 m*M* potassium phosphate buffer (pH 6.8) but they were retarded; ADP, ATP* and adenosine tetraphosphate were eluted at increasingly higher characteristic phosphate molarities

* Abbreviations: AMP = adenosine monophosphate; ADP = adenosine diphosphate; ATP = adenosine triphosphate.

with an almost linear relationship between the number of phosphates and the molarity (Fig. 3). This would indicate that the nucleoside phosphates are adsorbed via the phosphate groups (on to C crystal sites) and that the interval between the neighbouring phosphate groups on the polyphosphate chain fits satisfactorily with that between adsorption sites on the crystal surface.

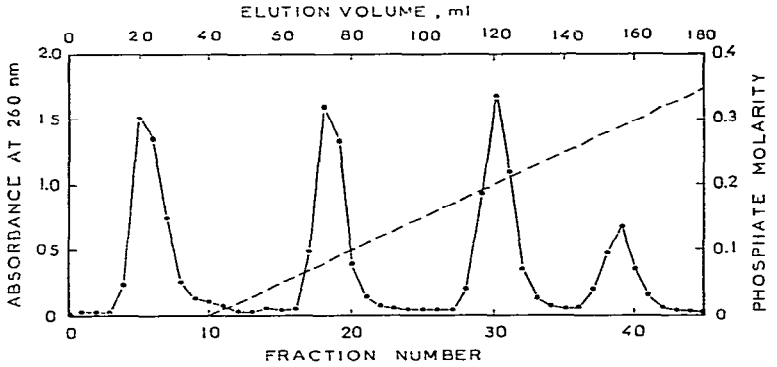

Fig. 3. Chromatography, at room temperature, of a mixture of AMP, ADP, ATP and adenosine tetraphosphate on a 10 × 1 cm HA column. The loading of about 2 mg of the mixture (in a small volume of 0.001 *M* potassium phosphate buffer, pH 6.8) was carried out at zero volume[12]; this amount (for a 10 × 1 cm column) would be small enough for the effect of mutual interactions among molecules adsorbed on HA or the mutual displacement of molecules[13] to be virtually negligible (*cf.*, Figs. 3–5 in ref. 14). Elution was carried out with a linear molarity gradient of potassium phosphate buffer (pH 6.8) (0.001–0.5 *M*; 100 + 100 ml), which was introduced after a volume of 4 ml had been eluted after loading, but which begins at 40 ml owing to the adsorption of the ions of the buffer on to the crystal surface (see Discussion); this was followed by refractometry and is indicated by the broken line-(right-hand ordinate). On the abscissa, both the fraction number and the elution volume are shown; the latter was estimated on the basis that the slope of the gradient of phosphate molarity should be 0.5/(100 + 100) = 0.0025 (*M*/ml) (*cf.*, Discussion). The yields were 133, 113, 113 and 50% for AMP, ADP, ATP and adenosine tetraphosphate, respectively, with an overall recovery of 102% (for an explanation of which, see Discussion). For necessary information involved in the figure, see Table II. (This figure is reproduced with slight modifications, from Fig. 1 in ref. 11, with the permission of Prof. G. Bernardi).

In this paper, on the basis of the Taves and Reedy model[1], an attempt is made to apply the theory developed in an earlier paper[7] to the experimental results of the chromatography of a mixture of AMP, ADP, ATP and adenosine tetraphosphate carried out by Bernardi[11], which is shown in Fig. 3, and to evaluate the adsorption energy per univalent phosphate group on the polyphosphate chain of the nucleotides. Some other experimental parameters are also evaluated. The reasonable results of the calculation strongly support the hypothesis that a hydroxyl position on the crystal surface corresponds to a chromatographic C site and the model for the manner of the adsorption of polyphosphate proposed by Taves and Reedy[1].

THEORETICAL

In an earlier paper[7], it was shown that, provided the activity of competing ions is proportional to the molarity, the elution molarity, m_{elu}, at the maximum height*

* Unless s is extremely small, it should be the elution molarity at the maximal height of the chromatographic peak that can be described by eqn. 15 in ref. 7 or eqn. 1 in this paper (see ref. 9).

of each chromatographic peak of a mixture with a small load can be described by eqn. 15 in ref. 7, or by

$$s = \frac{1}{(x' + 1)\cdot\varphi'\cdot\beta_3\,\sigma\,e^{x\varepsilon_3/kT}}\cdot[(\varphi'\cdot m_{elu} + 1)^{x'+1} - (\varphi'\cdot m_{in} + 1)^{x'+1}] \quad (1)$$

in which

$$s = g\,L \quad (2)$$

and

$$\varphi' = \frac{\Lambda_2}{m} \quad (3)$$

In eqn. 2, g is a constant representing the slope (molarity per unit column length) of the linear gradient of competing ions and L is the length of the column; in eqn. 3, Λ_2 is a parameter proportional to the activity of competing ions defined by eqn. 3 in ref. 7 and m is the corresponding molarity. Therefore, φ' is a constant assuming proportionality between the activity and the molarity. In eqn. 1, m_{in} is the molarity of competing ions in the initial buffer before the gradient is applied; x' is the number of sites of HA on which competing ions cannot be adsorbed owing to the presence of an adsorbed molecule; x is the number of adsorption groups of the molecule that can react with sites of HA; $-\varepsilon_3$ ($\varepsilon_3 > 0$) is the adsorption energy of an adsorption group of the molecule on to one of the sites of HA*; and σ and β_3 are constants related to the symmetry of the molecule** and to the property of the column, respectively.

Now, we propose a model for the adsorption of AMP, ADP, ATP and adenosine tetraphosphate on the HA surface as shown in Table I, in which ε'' is the adsorption energy (to one of the crystal sites) of a phosphate group of AMP or the terminal phosphate group of the polyphosphate chain of ADP, ATP and adenosine tetraphosphate; ε' is the adsorption energy for one univalent phosphate group on the polyphosphate chain of ADP, ATP and adenosine tetraphosphate; and x_0' is the number of sites of HA on which competing ions cannot be adsorbed owing to the presence of the terminal phosphate group plus the adenosine part of the nucleotide, assuming that a univalent phosphate on the polyphosphate chain covers only one crystal site. It seems also reasonable to assume that a terminal phosphate group covers only one crystal site, according to which $x_0' - 1$ indicates the number

* It is evident that the term $x\varepsilon_3$ in eqn. 1 can be re-written as $x_1\varepsilon' + x_2\varepsilon''$ if the molecule contains two types of adsorption groups with different adsorption energies, ε' and ε'', which is the case with nucleoside phosphate (*cf.*, Table I).

** In a following paper[15], it will be mentioned that the theory for rigid molecules can be extended to the general case of flexible molecules and that σ represents not only the symmetry but also the flexibility of the molecule. It is reasonable to consider that the molecule of nucleoside phosphate is not completely rigid. It also seems reasonable to assume, however, that the values of σ for AMP, ADP, ATP and adenosine tetraphosphate are almost equal, because except for the part of the molecule fixed on the crystal surface or the phosphate chain (see below), the structures of these molecules are identical.

TABLE I

CHROMATOGRAPHIC MODELS OF AMP, ADP, ATP AND ADENOSINE TETRAPHOSPHATE

In the last column, symbols indicating the phosphate elution molarities at the maximal height of the chromatographic peaks are also shown for ADP, ATP and adenosine tetraphosphate. AMP is not retained on the column, however (see Fig. 3).

Molecule	*Adsorption energy per molecule*	x'	*Phosphate elution molarity*
AMP	ε''	x'_0	Not retained on the column
ADP	$\varepsilon'' + \varepsilon'$	$x'_0 + 1$	$m_{\mathrm{elu(ADP)}}$
ATP	$\varepsilon'' + 2\varepsilon'$	$x'_0 + 2$	$m_{\mathrm{elu(ATP)}}$
Adenosine tetraphosphate	$\varepsilon'' + 3\varepsilon'$	$x'_0 + 3$	$m_{\mathrm{elu(AtetraP)}}$

of crystal sites covered by the adenosine group of the nucleoside phosphate. On the basis of this model, eqn. 1 can be re-written for ADP, ATP and adenosine tetraphosphate as

$$\beta\sigma e^{\varepsilon''/kT} = \frac{a}{(x'_0 + 2)\cdot\varphi'\cdot s_{(\mathrm{ADP})}\cdot e^{\varepsilon'/kT}} \tag{4}$$

$$\beta\sigma e^{\varepsilon''/kT} = \frac{b}{(x'_0 + 3)\cdot\varphi'\cdot s_{(\mathrm{ATP})}\cdot (e^{\varepsilon'/kT})^2} \tag{5}$$

and

$$\beta\sigma e^{\varepsilon''/kT} = \frac{c}{(x'_0 + 4)\cdot\varphi'\cdot s_{(\mathrm{AtetraP})}\cdot (e^{\varepsilon'/kT})^3} \tag{6}$$

respectively, in which

$$a = (\varphi'\cdot m_{\mathrm{elu(ADP)}} + 1)^{x'_0+2} - (\varphi'\cdot m_{\mathrm{in}} + 1)^{x'_0+2} \tag{7}$$

$$b = (\varphi'\cdot m_{\mathrm{elu(ATP)}} + 1)^{x'_0+3} - (\varphi'\cdot m_{\mathrm{in}} + 1)^{x'_0+3} \tag{8}$$

and

$$c = (\varphi'\cdot m_{\mathrm{elu(AtetraP)}} + 1)^{x'_0+4} - (\varphi'\cdot m_{\mathrm{in}} + 1)^{x'_0+4} \tag{9}$$

where the subscript AtetraP represents adenosine tetraphosphate. In eqns. 4–6, β is used instead of β_3; $s_{(\mathrm{ADP})}$, $s_{(\mathrm{ATP})}$ and $s_{(\mathrm{AtetraP})}$ are the effective values of s (eqn. 2) for ADP, ATP and adenosine tetraphosphate, respectively, which are equal to s provided that the R_F values before the gradient of phosphate ions is applied are exactly zero. Actually, however, these values [$R_{F,\mathrm{in(ADP)}}$, $R_{F,\mathrm{in(ATP)}}$ and $R_{F,\mathrm{in(AtetraP)}}$] must be slightly greater than zero and increase in the order $0 \lesssim R_{F,\mathrm{in(AtetraP)}} < R_{F,\mathrm{in(ATP)}} < R_{F,\mathrm{in(ADP)}}$, which means that the effective lengths [$L_{(\mathrm{ADP})}$, $L_{(\mathrm{ATP})}$ and $L_{(\mathrm{AtetraP})}$] of the column for these molecules are smaller than the actual length (L) and decrease in the

order of $L \gtrsim L_{(\mathrm{AtetraP})} > L_{(\mathrm{ATP})} > L_{(\mathrm{ADP})}$. This also means that $s \gtrsim s_{(\mathrm{AtetraP})} > s_{(\mathrm{ATP})} > s_{(\mathrm{ADP})}$ (see eqn. 2). Now, by eliminating $\beta\sigma e^{\varepsilon''/kT}$ between eqns. 4 and 5 and between eqns. 5 and 6, we obtain

$$e^{\varepsilon'/kT} = \frac{s_{(\mathrm{ADP})}}{s_{(\mathrm{ATP})}} \cdot \frac{x_0' + 2}{x_0' + 3} \cdot \frac{b}{a} \tag{10}$$

and

$$e^{\varepsilon'/kT} = \frac{s_{(\mathrm{ATP})}}{s_{(\mathrm{AtetraP})}} \cdot \frac{x_0' + 3}{x_0' + 4} \cdot \frac{c}{b} \tag{11}$$

Further, by eliminating $e^{\varepsilon'/kT}$ between eqns. 10 and 11, and by using eqn. 7, we obtain

$$m_{\mathrm{elu(ADP)}} = \frac{1}{\varphi'} \cdot \left\{ \left[\frac{s_{(\mathrm{ADP})} \cdot s_{(\mathrm{AtetraP})}}{s_{(\mathrm{ATP})^2}} \cdot \frac{(x_0' + 2) \cdot (x_0' + 4)}{(x_0' + 3)^2} \cdot \frac{b^2}{c} + \right. \right.$$

$$\left. \left. + (\varphi' \cdot m_{\mathrm{in}} + 1)^{x_0'+2} \right]^{\frac{1}{x_0'+2}} - 1 \right\} \tag{12}$$

Now, if the values of x_0', $s_{(\mathrm{ADP})}$, $s_{(\mathrm{ATP})}$, $s_{(\mathrm{AtetraP})}$, φ', m_{in}, $m_{\mathrm{elu(ATP)}}$ and $m_{\mathrm{elu(AtetraP)}}$ are known, then the values of $m_{\mathrm{elu(ADP)}}$ and $e^{\varepsilon'/kT}$ can be estimated by using eqn. 12 and eqn. 10 (or eqn. 11), respectively, which enables one to evaluate $\beta\sigma e^{\varepsilon''/kT}$ by using one of eqns. 4–6.

In order to estimate these values by using Fig. 3 or the information involved in it as shown in Table II, we consider the following successive approximation method. Let us introduce several hypothetical values such as 1, 2, 3, ... into x_0' and, as a first step of the successive approximation, let us assume that $s_{(\mathrm{ADP})} = s_{(\mathrm{ATP})} = s_{(\mathrm{AtetraP})} = s$ (see Table II). It should be noted that this assumption would be slightly different from the actual case in Fig. 3 but that it can be realized, if the gradient of phosphate ions can be applied immediately after loading of the sample is completed. We substitute the hypothetical values of x_0', $s_{(\mathrm{ADP})}$, $s_{(\mathrm{ATP})}$ and $s_{(\mathrm{AtetraP})}$ and the experimental values of m_{in}, $m_{\mathrm{elu(ATP)}}$ and $m_{\mathrm{elu(AtetraP)}}$ (see Table II) into eqn. 12, which now expresses $m_{\mathrm{elu(ADP)}}$ as a function of φ' only. Fig. 4 illustrates the dependence of $m_{\mathrm{elu(ADP)}}$ on $\log_{10} \varphi'$ for different values of x_0'. It can be seen that there exists a finite value of φ' which gives $m_{\mathrm{elu(ADP)}}$ a minimal value and that $m_{\mathrm{elu(ADP)}}$ tends to different finite values when φ' tends to zero (*i.e.*, $\log_{10} \varphi'$ tends to $-\infty$) and $+\infty$, respectively, or we can write

$$\lim_{\varphi' \to 0} m_{\mathrm{elu(ADP)}} = \frac{s_{(\mathrm{ADP})} \cdot s_{(\mathrm{AtetraP})}}{s_{(\mathrm{ATP})}^2} \cdot \frac{[m_{\mathrm{elu(ATP)}} - m_{\mathrm{in}}]^2}{m_{\mathrm{elu(AtetraP)}} - m_{\mathrm{in}}} + m_{\mathrm{in}} \tag{13}$$

and

$$\lim_{\varphi' \to +\infty} m_{\mathrm{elu(ADP)}} = \left\{ \frac{s_{(\mathrm{ADP})} \cdot s_{(\mathrm{AtetraP})}}{s_{(\mathrm{ATP})}^2} \cdot \frac{(x_0' + 2) \cdot (x_0' + 4)}{(x_0' + 3)^2} \times \right.$$

$$\left. \times \frac{[m_{\mathrm{elu(ATP)}}^{x_0'+3} - m_{\mathrm{in}}^{x_0'+3}]^2}{m_{\mathrm{elu(AtetraP)}}^{x_0'+4} - m_{\mathrm{in}}^{x_0'+4}} + m_{\mathrm{in}}^{x_0'+2} \right\}^{\frac{1}{x_0'+2}} \tag{14}$$

TABLE II

INFORMATION INVOLVED IN FIG. 3

Parameter	*Symbol*	*Information*
Column length	L	10 (cm)
Column diameter	$\varnothing$	1 (cm)
Slope of phosphate molarity gradient (in molarity per unit elution volume)	grad	0.0025 (M/ml)
Interstitial volume per unit length of the column	v	0.628 (ml/cm)*
Total interstitial volume of the column	V_T	6.28 (ml)
Slope of phosphate molarity gradient (in molarity per unit column length)	g	0.00157 (M/cm)**
Product of g and L	s	0.0157 (M)
Molarity of phosphate ions before the gradient begins	m_{in}	0.001 (M)***
Volume of the solvent eluted from sample loading until the gradient begins	V'	40 (ml)
Temperature	T	Room temperature§
Elution volume at the maximal height of AMP chromatographic peak	$V_{(AMP)}$	20 (ml)
B or R_F value at the maximal height of AMP peak	$B_{in(AMP)}$ or $R_{F,\ in(AMP)}$	0.314§§
Phosphate elution molarity at the maximal height of ADP peak	$m_{elu(ADP)}$	0.08_3 (M)
Phosphate elution molarity at the maximal height of ATP peak	$m_{elu(ATP)}$	0.20_0 (M)
Phosphate elution molarity at the maximal height of adenosine tetraphosphate peak	$m_{elu(AtetraP)}$	0.28_7 (M)

* Calculated by the relationship $v = \varnothing^2/4 \cdot \pi \cdot 0.8 = 0.628\ \varnothing^2$, where the factor 0.8 is the ratio of the interstitial volume to the total packed volume of HA estimated by Bernardi[16].

** Calculated by the relationship $g = v \cdot \text{grad}$.

*** This is not precisely the experimental value, but it must be close to the true value (see Discussion).

§ The value of ε' is estimated by assuming that room temperature is 25° (see Table IV).

§§ Calculated by the relationship $B_{in(AMP)}$ or $R_{F,\ in(AMP)} = V_T/V_{(AMP)}$ (*cf.*, eqn. 20).

It is evident that, in order for φ' to have a physical meaning, $\varphi' > 0$ (see eqn. 3).

Now, in order for eqn. 12 to have a physical meaning, there must be a one-to-one correspondence between $m_{elu(ADP)}$ and φ', which is evident because if the "activity coefficient" φ' (see eqn. 3) is given, $m_{elu(ADP)}$ should be defined uniquely, while, for $m_{elu(ADP)}$ to be defined, φ' must have a unique value. This means that the part of each curve in Fig. 4 which can have a physical meaning is either the point at which m_{elu} is at a minimum or the region in which $\lim_{\varphi' \to +\infty} m_{elu} < m_{elu} < \lim_{\varphi' \to 0} m_{elu}$. The latter possibility can be excluded, because, provided that this is the situation, it is possible that, when φ' varies (for instance, by the addition of an organic solvent to the system), $m_{elu(ADP)}$ varies but that both $m_{elu(ATP)}$ and $m_{elu(AtetraP)}$ continue to have constant values. This is due to the fact that the shape of each curve in Fig. 4 is constant provided that both $m_{elu(ATP)}$ and $m_{elu(AtetraP)}$ are constant, which is not the actual situation. The reason why the mathematical expression, eqn. 12, involves physically meaningless relationships is evident because, if $m_{elu(ADP)}$, $m_{elu(ATP)}$ and $m_{elu(AtetraP)}$ are given, eqn. 12 can be considered as the equation for φ'; this should be soluble (provided that it has solutions) whatever combinations among the values of $m_{elu(ADP)}$, $m_{elu(ATP)}$ and

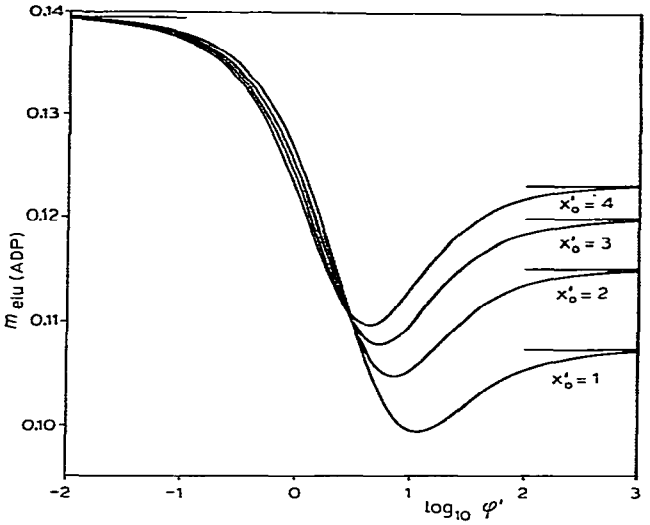

Fig. 4. $m_{elu(ADP)}$ as a function of $\log_{10}\varphi'$ for several values of x'_0 calculated in the first cycle of the successive approximations. Two asymptotes obtained when $\log_{10}\varphi'$ tends to both $-\infty$ and $+\infty$ are also shown for each curve of $m_{elu(ADP)}$ (for details, see text).

$m_{elu(AtetraP)}$ may be assumed; it is only one of these combinations that can have a physical meaning. Hence, the elution molarity of ADP must be written as

$$m_{elu(ADP)} = \min_{\varphi'} \left(\frac{1}{\varphi'} \cdot \left\{ \left[\frac{s_{(ADP)} \cdot s_{(AtetraP)}}{s_{(ATP)}^2} \cdot \frac{(x'_0 + 2)\cdot(x'_0 + 4)}{(x'_0 + 3)^2} \cdot \frac{b^2}{c} + \right. \right. \right.$$

$$\left. \left. \left. + (\varphi' \cdot m_{in} + 1)^{x'_0+2} \right]^{\frac{1}{x'_0+2}} - 1 \right\} \right) \qquad (15)$$

from which the value of φ' can be determined at the same time. In the Appendix, we give a mathematical proof for a more general relationship than eqn. 15:

$$\left(\frac{\partial M_1}{\partial \varphi'} \right)_{M_2, M_3} = 0 \qquad (15')$$

where M_1, M_2 and M_3 represent any one of $m_{elu(ADP)}$, $m_{elu(ATP)}$ and $m_{elu(AtetraP)}$, respectively.

The following step of the calculation is to substitute the values of $m_{elu(ADP)}$ and φ' obtained from eqn. 15 into eqn. 10, or only the latter value into eqn. 11, which gives the value of $e^{\varepsilon'/kT}$. We then substitute $m_{elu(ADP)}$ or the experimental value of either $m_{elu(ATP)}$ or $m_{elu(AtetraP)}$, the experimental value of m_{in} and the hypothetical values of x'_0 and $s_{(ADP)}$, $s_{(ATP)}$ or $s_{(AtetraP)}$ into eqn. 4, 5 or 6, which now gives the value of $\beta\sigma e^{\varepsilon''/kT}$. By using this value of $\beta\sigma e^{\varepsilon''/kT}$, we can calculate the values of B or R_F (see ref. 7), B_{in} or $R_{F,in}$, in the initial state of the chromatography before the gradient is

applied (in which the phosphate molarity is m_{in}) for AMP, ADP, ATP and adenosine tetraphosphate, respectively, by the following relationships (*cf.*, eqn. 1 in ref. 7):

$$B_{in(AMP)} = R_{F,in(AMP)} = \frac{1}{1 + \beta\sigma e^{\varepsilon''/kT} (\varphi' m_{in} + 1)^{-x_0'}} \tag{16}$$

$$B_{in(ADP)} = R_{F,in(ADP)} = \frac{1}{1 + \beta\sigma e^{\varepsilon''/kT} e^{\varepsilon'/kT} (\varphi' m_{in} + 1)^{-x_0'-1}} \tag{17}$$

$$B_{in(ATP)} = R_{F,in(ATP)} = \frac{1}{1 + \beta\sigma e^{\varepsilon''/kT} (e^{\varepsilon'/kT})^2 (\varphi' m_{in} + 1)^{-x_0'-2}} \tag{18}$$

and

$$B_{in(AtetraP)} = R_{F,in(AtetraP)} = \frac{1}{1 + \beta\sigma e^{\varepsilon''/kT} (e^{\varepsilon'/kT})^3 (\varphi' m_{in} + 1)^{-x_0'-3}} \tag{19}$$

It follows from eqn. 16 that the theoretical value of the elution volume of AMP, $V_{(AMP)}$, is

$$V_{(AMP)} = \frac{V_T}{R_{F,in(AMP)}} \tag{20}$$

where V_T is the total interstitial volume of the column (see Table II). The effective lengths of the column and the effective values of s for ADP, ATP and adenosine tetraphosphate can be calculated, by using eqns. 17–19, respectively, as

$$L_{(ADP)} = L - \frac{V'}{v} \cdot R_{F,in(ADP)} \tag{21}$$

$$L_{(ATP)} = L - \frac{V'}{v} \cdot R_{F,in(ATP)} \tag{22}$$

$$L_{(AtetraP)} = L - \frac{V'}{v} \cdot R_{F,in(AtetraP)} \tag{23}$$

$$s_{(ADP)} = g L_{(ADP)} \tag{24}$$

$$s_{(ATP)} = g L_{(ATP)} \tag{25}$$

and

$$s_{(AtetraP)} = g L_{(AtetraP)} \tag{26}$$

where V' is the volume of the initial buffer eluted from loading the sample until the gradient begins (see Table II) and v is the interstitial volume per unit length of the column (see Table II).

The first cycle of the successive approximation is now finished. The second

cycle begins by substituting the values of $s_{(ADP)}$, $s_{(ATP)}$ and $s_{(AtetraP)}$ obtained by eqns. 24–26 into eqn. 15, and the values of $m_{elu(ADP)}$, φ', $V_{(AMP)}$, $s_{(ADP)}$, $s_{(ATP)}$, $s_{(AtetraP)}$, etc., are again calculated through eqns. 15–26. These values must be slightly different from the values calculated in the preceding cycle. The discrepancy between the values obtained in the nth and the $n-1$th cycles must tend to zero when the value of n increases, however. Hence, the theoretical values of $m_{elu(ADP)}$, φ', $V_{(AMP)}$ [or $R_{F,in(AMP)}$], etc., can finally be estimated for each hypothetical value of x'_0. The values of $m_{elu(ADP)}$ and $V_{(AMP)}$ [or $R_{F,in(AMP)}$] are compared with the experimental values (see Table II) and the value of x'_0 is determined, from which it follows that the values of φ', $e^{\varepsilon'/kT}$ (or ε'), $\beta\sigma e^{\varepsilon''/kT}$, $B_{in(AMP)}$ [or $R_{F,in(AMP)}$], $B_{in(ADP)}$ [or $R_{F,in(ADP)}$], $B_{in(ATP)}$ [or $R_{F,in(ATP)}$], $B_{in(AtetraP)}$ [or $R_{F,in(AtetraP)}$], $L_{(ADP)}$, $L_{(ATP)}$, $L_{(AtetraP)}$, $s_{(ADP)}$, $s_{(ATP)}$ and $s_{(AtetraP)}$ are finally estimated. Fig. 5 summarizes the method for the evaluation of these parameters.

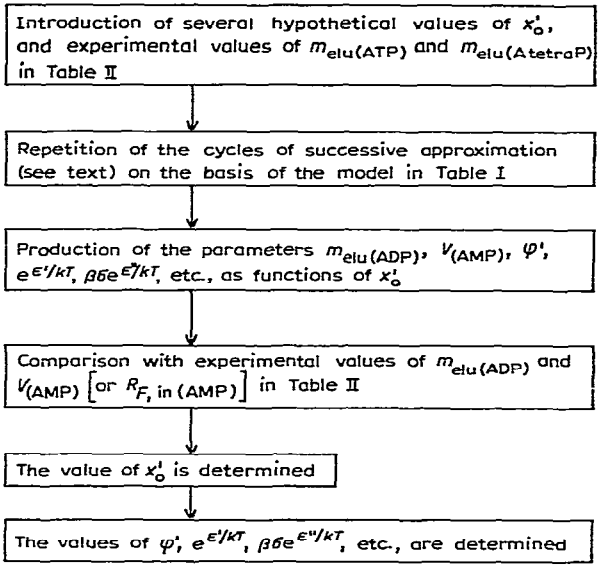

Fig. 5. Method for the estimation of the values of x_0, φ', $e^{\varepsilon'/kT}$, $\beta\sigma e^{\varepsilon''/kT}$, etc.

RESULTS OF CALCULATIONS

Table III shows values of φ', $m_{elu(ADP)}$ and $V_{(AMP)}$ calculated in the first to sixth cycles of the successive approximation for the case when $x'_0 = 2$, in which it can be seen that six cycles are sufficient to give good enough fits of the values with those obtained in the preceding cycle. Similar calculations were carried out assuming $x'_0 =$ 1, 3, 4, 5, 6 and 7. In all instances, six cycles were sufficient to give good fits. Fig. 6 illustrates $m_{elu(ADP)}$ as a function of $\log_{10} \varphi'$ obtained through eqn. 12 in the last of the six cycles for $x'_0 = 1$–4. The value of $m_{elu(ADP)}$ with a physical meaning is at the minimum of each curve (see Theoretical). In Fig. 6, the experimental value of $m_{elu(ADP)}$ [0.083 M (see Table II)] is also shown; this is closest to the minimum of the curve with $x'_0 = 2$ (0.087 M), but also close to the minimum of the curve with $x'_0 = 1$ (0.077 M).

TABLE III

VALUES OF φ', $m_{elu(ADP)}$ AND $V_{(AMP)}$ CALCULATED IN THE FIRST TO THE SIXTH CYCLES OF THE SUCCESSIVE APPROXIMATION FOR THE CASE WHEN $x'_0 = 2$

Number of cycle	φ'	$m_{elu(ADP)}$ *(M)*	$V_{(AMP)}$ *(ml)*
1	7.3	0.1048	20.5
2	4.6	0.0873	24.6
3	4.3	0.0844	27.6
4	4.6	0.0866	27.2
5	4.6	0.0870	26.7
6	4.6	0.0866	26.7

On the other hand, it can be shown that the experimental value of $V_{(AMP)}$ [20 ml (see Table II)] is closest to the theoretical value obtained assuming $x'_0 = 1$ (22 ml) and next to the value corresponding to $x'_0 = 2$ (27 ml). Table IV summarizes the values of several parameters finally determined for both $x'_0 = 1$ and $x'_0 = 2$.

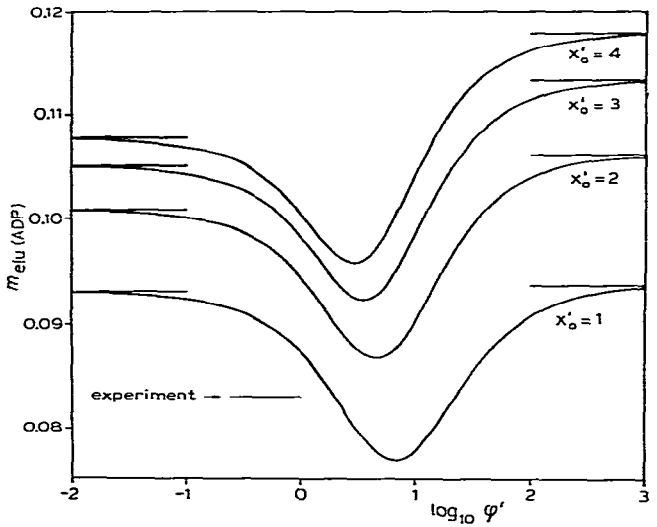

Fig. 6. $m_{elu(ADP)}$ as a function of $\log_{10} \varphi'$ for several values of x'_0 calculated in the last of the six cycles of the successive approximation. Two asymptotes obtained when $\log_{10} \varphi'$ tends to both $-\infty$ and $+\infty$ are also shown for each curve of $m_{elu(ADP)}$. The minimum of each curve gives the theoretical value of $m_{elu(ADP)}$. It can be seen that the best fit with the experiment is obtained when $x'_0 = 2$ (for details, see text).

DISCUSSION

All calculations were carried out by assuming that the molarity, m_{in}, of phosphate ions before the gradient begins is equal to the molarity of both the solvent of the sample solution and the starting buffer with which the gradient was made, *i.e.*, 0.001 *M* (see legend of Fig. 3). In the experiment in Fig. 3, however, the gradient of phosphate ions was introduced into the column after a volume of only 4 ml had been eluted after loading (which was done at zero volume; see legend of Fig. 3), and it can

TABLE IV

ESTIMATED VALUES OF SEVERAL EXPERIMENTAL PARAMETERS FOR $x_0' = 1$ AND $x_0' = 2$

Parameter	x_0'		*Parameter*	x_0'	
	1	*2*		*1*	*2*
φ'	6.7	4.6	$B_{in(ATP)}$ or $R_{F,in(ATP)}$	0.013	0.013
$e^{\varepsilon'/kT}$	5.45	4.80	$B_{in(AtetraP)}$ or $R_{F,in(AtetraP)}$	0.0025	0.0028
ε'/kT	1.70	1.57	$L_{(ADP)}$ (cm)	5.6	6.2
ε' (kcal/mole)*	1.00	0.93	$L_{(ATP)}$ (cm)	9.1	9.2
$\beta\sigma e^{\varepsilon''/kT}$	2.53	3.29	$L_{(AtetraP)}$ (cm)	9.8	9.8
$B_{in(AMP)}$ or $R_{F,in(AMP)}$	0.28	0.23	$s_{(ADP)}$ (M)	0.0089	0.0097
$B_{in(ADP)}$ or $R_{F,in(ADP)}$	0.068	0.060	$s_{(ATP)}$ (M)	0.0144	0.0144
			$s_{(AtetraP)}$ (M)	0.0155	0.0154

* Calculated assuming that $T = 25°$.

be seen that the gradient begins at an elution volume of 40 ml or that the volume of the solvent eluting between the introduction and the beginning of the gradient is 36 ml, which is much larger than the total interstitial volume of the column, *i.e.*, 6.28 ml (see Table II). This would indicate that the gradient is delayed owing to the adsorption of the ions of the buffer on to HA. On the other hand, it can generally be observed that the actual slope of the gradient is virtually equal to the slope that would be realized if there were no adsorption of the ions on the crystal surface*; this means that the delay of the gradient occurs immediately after the gradient is introduced and that, after the initial delay, any part of the gradient migrates with the same rate and $R_F = 1$. This may be due to the fact that the concentration of the ions in the interstices of the column is extremely high and virtually independent of the adsorption on to the crystal surface (except just at the beginning of the gradient). In Fig. 3, it is difficult to know the exact molarity of the phosphate between the introduction and the beginning of the gradient; this must be small because refractometry shows it to be virtually zero[12], but it is probably higher than 0.001 *M*. Eqns. 16–19 show that the values of $R_{F,in}$ vary only very slightly with a variation in the value of m_{in}, provided, however, that $\varphi' \cdot m_{in} \ll 1$.

It is also assumed that the adsorption of a molecule on the surface of HA is unique; this is correct if a particular orientation of the molecule on the crystal surface is energetically much more stable than the other possible orientations, and could be applied approximately to all nucleoside phosphates in Fig. 3. However, the exactness of the approximation must be different for different molecules and it must be better following the order of the values of the adsorption energies in the most stable orientation, *i.e.*, following the order adenosine tetraphosphate, ATP, ADP and AMP. According to this consideration, the theoretical values of $V_{(AMP)}$ and $m_{elu(ADP)}$ estimated on the basis of the approximation of the unique adsorption of the molecule and by using the experimental values of both $m_{elu(ATP)}$ and $m_{elu(AtetraP)}$ (see Table II) might

* In the experiment in Fig. 3, however, it was reported[11] that the volume of each chromatographic fraction is 3 ml. If the slope of the gradient is calculated by using this value, it becomes slightly larger. This must be due to the fact that the measurement of the fraction volume is not exact[12].

be slightly larger than the corresponding experimental values; this suggests that the value 2 estimated for x_0' is more probable than the value 1 because, if $x_0' = 2$, both the theoretical values of $m_{elu(ADP)}$ (0.087 M) and $V_{(AMP)}$ (27 ml) are larger than the corresponding experimental values [$m_{elu(ADP)} = 0.083$ M and $V_{(AMP)} = 20$ ml], whereas if $x_0' = 1$, the theoretical value of $m_{elu(ADP)}$ (0.077 M) is smaller than the experimental value (see Results of calculations). On the other hand, however, a similar experiment for poly-L-lysine suggests that the theoretical value of $m_{elu(ADP)}$ would be slightly smaller than the experimental value owing to a slight deviation from linearity of the relationship between A_2 and m (see ref. 15).

In this step, it is difficult to determine the exact value of x_0'. However, a value of 1–2 estimated for x_0', which would indicate that the adenosine group of adsorbed nucleosides covers at most only one crystal C site (see Theoretical), seems reasonable and consistent with the hypothesis that a C site corresponds to a void of the hydroxyl ion of HA (see Introduction). The value (0.9–1 kcal/mole) estimated for ε' or the adsorption energy for a univalent phosphate group on the polyphosphate chain of the nucleotide (Table IV) is also reasonable and about twice the value (0.5 kcal/mole) estimated for a carboxyl group on the basis of the microheterogeneous model of tropocollagen[17]. As these reasonable conclusions were reached on the basis of the assumption that each phosphate group on the polyphosphate chain should be adsorbed on a C site with a good fit between the intervals of neighbouring phosphate groups and neighbouring C sites, and as the good fit of the intervals would be possible only if a C site corresponds to a hydroxyl position of HA (see Introduction), it can be concluded that these results verify the hypothesis of the one-to-one correspondence between a C site and a hydroxyl position (void of the hydroxyl ion).

Jung *et al.*[18] suggested, however, from adsorption experiments with inorganic pyrophosphate and two diphosphonates (containing a P–C–P structure in contrast to a P–O–P structure in pyrophosphate), namely disodium ethane-1-hydroxy-1,1-diphosphonate (EHDP) and disodium dichloromethylene diphosphonate (Cl_2MDP), the existence of not only a common binding site but also a separate site preferential for pyrophosphate. This suggestion is justified[18] by the following arguments: (a) A Scatchard plot (a plot of the ratio of the number of molecules bound to the free concentration in solution as a function of the amount bound) shows that the affinity constant of the first class of sites is highest for EHDP, followed by pyrophosphate, and smallest for Cl_2MDP; but the index for the total binding capacity is largest for pyrophosphate, followed by EHDP and smallest for Cl_2MDP*. When the concentration of pyrophosphate in solution (pH 7.4) is high, a binding of about two molecules per surface unit cell of HA can be estimated (under some assumptions, of course); this is greater than the value predicted by the model of Taves and Reedy[1] (see Introduction). (b) The addition of EHDP displaces pyrophosphate previously bound on HA, but when EHDP is added in amounts up to 50% of the pyrophosphate previously present on the HA, the displaced pyrophosphate and the added EHDP are in molar proportions of 1:3. For larger amounts of EHDP, the relative displacement of

* It is necessary, however, to be careful enough about how the mutual interactions among molecules adsorbed on the surface of HA[13] influence the values obtained through the Scatchard plot, which would indicate, in the ideal case, the affinity of molecule for HA and the binding capacity of HA.

pyrophosphate decreases. These observations are consistent with the existence of two types of adsorption sites*. It can be considered, however, that chromatography reflects mainly the state where the density of molecules on the crystal surface is small enough, because the development of molecules is possible only when the density is small, the state where a considerable proportion of molecules in a section of the column is in solution being realized when the density is small. In this state, the strongest site must be used mainly for the adsorption of molecules, and this must be the C site.

It was shown by Krane and Glimcher[10] that synthetic apatite crystals form complexes with various nucleoside tri- and diphosphates as well as inorganic pyrophosphate at physiological temperature and pH. The terminal phosphorus atom of the bound nucleotide was transferred to a crystal surface phosphate with the formation of pyrophosphate on the crystal and the respective nucleoside di- and monophosphate. It was also shown by Krane and Glimcher[10] that the susceptibility to inorganic pyrophosphatase of the pyrophosphate bound to the crystal was different, depending on whether the pyrophosphate was bound as such from solution (82% hydrolysed) or whether it was formed from the transphosphorylation reaction with ATP (16% hydrolysed). On the other hand, when the crystals from both types of experiment were dissolved and the pyrophosphate was isolated and allowed to react with pyrophosphatase, essentially all of the inorganic pyrophosphate was converted into inorganic orthophosphate. Krane and Glimcher suggested[10] that this difference in enzymatic susceptibility is due to a different orientation of the pyrophosphate on the surface of the HA, depending on the origin of the pyrophosphate. A reasonable atomic explanation was given by Taves and Reedy[1], who considered that the position of the resulting pyrophosphate from the transphosphorylation reaction is roughly perpendicular rather than parallel to the $\vec{c}$ axis of HA. It was reported by Bernardi[11] that the chromatography of a mixture of AMP, ADP, ATP and adenosine tetraphosphate on an HA column (Fig. 3) gave yields of 133, 113, 113 and 50%, respectively. It is probable that this is due to the fact that the terminal phosphorus of the bound nucleoside di-, tri- and tetraphosphates was partially transferred to a crystal surface phosphate with the formation of pyrophosphate on the crystal and the respective nucleoside mono-, di- and triphosphate.

Another example of the molecular reaction that is catalysed by HA on its crystal surface is the degradation of RNA at a high temperature (70°), reported by Martinson and Wagenaar[19]. In this instance, it is considered[19] that the crystal surface of HA is not directly involved in the degradation of RNA but that the degradation is due to a presumably very high concentration of Ca^{2+} ions near the crystal surface, perhaps held there by the requirement of electrostatic charge balance. It was also reported[19] that there is no detectable degradation in the case of DNA, which is consistent with the work of Bernardi[20], who showed that, at room temperature, no significant changes in the physical, chemical and biological properties of native DNA take place upon the adsorption–elution process on HA columns.

Finally, the value of the parameter φ' (4.6–6.7) estimated in this work (Table IV) for competing phosphate ion is comparable to the value of 5 estimated in earlier work[7] for competing potassium ion [see Fig. 2 (e) in ref. 7]. However, this value is

* The possibility that the second type of crystal site corresponds to a P site[7,8] can almost be excluded, because this site reacts with the basic group of the molecule.

much larger than the value of 0.6 estimated for phosphate ion[7], which was based on the experimental data for tropocollagen (Fig. 5 in ref. 7); it was shown that $x'\varphi' = 179$, and the value of 300 estimated for the parameter x' for tropocollagen by assuming that no C sites under the adsorbed molecule can react with phosphate ions*. The estimation of the value of x', which is based on the well known molecular dimensions and shape of tropocollagen, must be correct at least in its order of magnitude, whereas if the value of 4.6–6.7 for the parameter φ' estimated in this work is substituted into the relationship $x'\varphi' = 179$, one obtains $x' = 27$–39; this is much less than 300. Tropocollagen is a rod-like molecule with three polypeptide chains forming a triple helix, which involves mainly glycyl and imino residues occupying 1/3 and 1/5–1/4 of the total residues, respectively; it is considered that the conformation of the triple helix is similar to that of $(\text{Gly–Pro–Pro})_n$ (see ref. 21). As glycyl residues occupying 1/3 of the total residues have no side-chains, it might be possible that phosphate ions of the buffer can enter the spaces among presumably protruding side-chains of aspartic and glutamic residues under the adsorbed molecule, carboxyl groups of which are reacting with C sites; this would reduce considerably the value of x'. In a following paper[15], it will be shown that it is probable that competing ions can enter the spaces among protruding side-chains of poly-L-lysine, ε-amino groups of which are reacting with P sites[7,8] of HA. One cannot, however, exclude the possibility that the adsorption of phosphate ions on to the molecular surface of tropocollagen, if it occurs to a high extent, changes the apparent values of x'.

APPENDIX

A mathematical proof for eqn. 15′ is given below. According to our chromatographic model, it can be considered that, under any experimental condition where φ' has a constant value, M_1, M_2 and M_3 are functions of two parameters (concerning the property of the sample molecule) ε' and $\varepsilon^* \equiv \varepsilon'' + kT \log \sigma$ if x_0' is given, respectively, or it can be written

$$M_1 = \mathrm{f}_1(\varepsilon', \varepsilon^*) \tag{A1}$$

$$M_2 = \mathrm{f}_2(\varepsilon', \varepsilon^*) \tag{A2}$$

$$M_3 = \mathrm{f}_3(\varepsilon', \varepsilon^*) \tag{A3}$$

Now, eliminating ε' and ε^* among eqns. A1–A3, one has

$$M_1 = F(M_2, M_3) \tag{A4}$$

or

$$\mathrm{d}M_1 = \frac{\partial F}{\partial M_2} \cdot \mathrm{d}M_2 + \frac{\partial F}{\partial M_3} \cdot \mathrm{d}M_3 \tag{A5}$$

* It can be considered that tropocollagen is adsorbed on to C sites by using carboxyl groups of aspartic and glutamic residues[7]. These residues occupy about one tenth of the total residues.

As the function F involves φ' as a parameter, it is possible to re-write eqns. A4 and A5, respectively, as

$$M_1 = \Phi(\varphi'; M_2, M_3) \tag{A6}$$

and

$$\mathrm{d}M_1 = \left(\frac{\partial \Phi}{\partial M_2}\right)_{\varphi', M_3} \mathrm{d}M_2 + \left(\frac{\partial \Phi}{\partial M_3}\right)_{\varphi', M_2} \mathrm{d}M_3 \tag{A7}$$

On the other hand, it is possible to consider that eqn. A6 has the form

$$M_1 = \Phi[\varphi', M_2(\varphi'), M_3(\varphi')] \tag{A8}$$

from which we can derive

$$\mathrm{d}M_1 = \left(\frac{\partial \Phi}{\partial \varphi'}\right)_{M_2, M_3} \mathrm{d}\varphi' + \left(\frac{\partial \Phi}{\partial M_2}\right)_{\varphi', M_3} \mathrm{d}M_2 + \left(\frac{\partial \Phi}{\partial M_3}\right)_{\varphi', M_2} \mathrm{d}M_3 \tag{A9}$$

Now, by comparing eqn. A9 with eqn. A7, it can be concluded that

$$\left(\frac{\partial \Phi}{\partial \varphi'}\right)_{M_2, M_3} = 0 \tag{A10}$$

which is eqn. 15′. It should be noted that $(\partial \Phi)_{M_2, M_3}$ is a virtual displacement.

ACKNOWLEDGEMENTS

The author is grateful to Dr. G. Bernardi for useful discussions and interest in this work, and thanks the Délégation Générale à la Recherche Scientifique et Technique, Paris, for financial support. Calculations were performed on the CDC 6600 computer of the Faculty of Sciences, University of Paris.

REFERENCES

1 D. R. Taves and R. C. Reedy, *Calcif. Tissue Res.*, 3 (1969) 284.
2 M. A. Kay, R. A. Young and A. S. Posner, *Nature (London)*, 204 (1964) 1050.
3 K. Sudarsanan and R. A. Young, *Acta Crystallogr.*, B25 (1969) 1534.
4 J. C. Elliott, P. E. Mackie and R. A. Young, *Science*, 180 (1973) 1055.
5 W. E. Brown, *Nature (London)*, 196 (1962) 1048.
6 D. R. Taves, *Nature (London)*, 200 (1963) 1312.
7 T. Kawasaki, *J. Chromatogr.*, 93 (1974) 313.
8 T. Kawasaki, *J. Chromatogr.*, 93 (1974) 337.
9 T. Kawasaki, *J. Chromatogr.*, 120 (1976) 271.
10 S. M. Krane and M. J. Glimcher, *J. Biol. Chem.*, 237 (1962) 2991.
11 G. Bernardi, *Biochim. Biophys. Acta*, 91 (1964) 686.

12 G. Bernardi, unpublished data.
13 T. Kawasaki, *J. Chromatogr.*, 82 (1973) 167.
14 T. Kawasaki and G. Bernardi, *Biopolymers*, 9 (1970) 257.
15 T. Kawasaki, in preparation.
16 G. Bernardi, *Methods Enzymol.*, 21 (1971) 95.
17 T. Kawasaki, *J. Chromatogr.*, 82 (1973) 237.
18 A. Jung, S. Bisaz and H. Fleish, *Calcif. Tissue Res.*, 11 (1973) 269.
19 H. G. Martinson and E. B. Wagenaar, *Biochemistry*, 13 (1974) 1641.
20 G. Bernardi, *Biochim. Biophys. Acta*, 174 (1969) 423.
21 W. Traub and K. Piez, *Advan. Protein Chem.*, 25 (1971) 243.